Available online at www.sciencedirect.com
ScienceDirect
Journal of Solid State Chemistry 180 (2007) 805–811
JOURNAL OF SOLID STATE CHEMISTRY
www.elsevier.com/locate/jssc

Synthesis, crystal and band structures, and properties of a new supramolecular complex $(Hg_2As)_2(CdI_4)$

Jian-Ping Zou[a,b], Dong-Sheng Wu[a], Shu-Ping Huang[a], Jing Zhu[a], Guo-Cong Guo[a,*], Jin-Shun Huang[a]

[a]*State Key Laboratory of Structural Chemistry, Fujian Institute of Research on the Structure of Matter, Chinese Academy of Sciences, Fuzhou, Fujian 350002, PR China*

[b]*Graduate School, Chinese Academy of Sciences, Beijing 100039, PR China*

Received 7 September 2006; received in revised form 31 October 2006; accepted 31 October 2006
Available online 18 November 2006

Abstract

A new quaternary supramolecular complex $(Hg_2As)_2$ (CdI_4) (**1**) has been prepared by the solid-state reaction and structurally characterized by single crystal X-ray diffraction analysis. Compound **1** crystallizes in the space group $P2_1$ of the monoclinic system with two formula units in a cell: $a = 7.945(4)$, $b = 12.934(6)$, $c = 8.094(4)$ Å, $\beta = 116.898°(1)$, $V = 741.7(6)$ Å^3. The structure of **1** is characterized by a tridymite-like three-dimensional cationic framework, which is composed of mercury and arsenic atoms, with the channels being occupied by discrete CdI_4^{2-} tetrahedral guest-anions. The optical properties were investigated in terms of the diffuse reflectance and Fourier transform infrared spectra. The electronic band structure along with density of states (DOS) calculated by DFT method indicates that the present compound is a semiconductor with a direct band gap, and that the optical absorption is mainly originated from the charge transitions from I-5*p* and As-4*p* to Cd-5*s* and Hg-6*s* states.

Keywords: Band structure; Energy gap; Pnictide; Optical properties; Solid-state reaction; Supramolecular chemistry

1. Introduction

Pnictides have been investigated extensively because of their structural diversity and physical properties for the past 40 years. Among them, cadmium and mercury pnictidehalides are well attractive in inorganic chemistry and advanced material research because of their abundant structural features and distinctive electronic properties [1]. For instance, the propensity of mercury to linear two-coordination or to tetrahedral coordination can be exploited in the design of extended frameworks. As a rule, the topology with the formula of $(Hg_6Z_4)^{4+}$ (Z = P, As, Sb) [2] possesses cavities of two different sizes in close proximity that are capable of trapping guests of two different types. As another important example, the analogues of the well-known Millon's base salts [3] are composed of the cationic frameworks with the formula of $(Hg_2Z)^+$ (Z = P, As) that adopt a tridymite topology filled with different tetrahedral anions, such as $(HgBr_4)^{2-}$ [4] or $(ZnI_4)^{2-}$ [5]. Unlike the first type of the topology with the formula of $(Hg_6Z_4)^{4+}$, where there are more than 20 supramolecular complexes have been synthesized, only three examples of the second type, including $(Hg_2P)_2(HgBr_4)$ [4], $(Hg_2P)_2(ZnI_4)$ [5a] and $(Hg_2As)_2(ZnI_4)$ [5b], have been reported in the literature. Usually, on the basis of the nature of the different guests, the supramolecular complexes exhibit different electronic structures and diverse physical and chemical properties [2]. However, to the best of our knowledge, the optical and thermal properties, and the electronic band structures of cadmium and mercury pnictidehalides have been rarely reported in the literatures [1b,c,g].

Recently, we have begun a systematic investigation of mercury pnictide-based mixed-framework compounds to further explore new self-assembly supramolecular

*Corresponding author. Fax: +86 591 83714946.
E-mail address: gcguo@ms.fjirsm.ac.cn (G.-C. Guo).

0022-4596/$ - see front matter © 2006 Elsevier Inc. All rights reserved.
doi:10.1016/j.jssc.2006.11.018

materials. The idea is to exploit 3-D cationic host topology and guest anions to form various supramolecular structures. Because the II–V group compounds have good semiconducting and thermoelectric properties [6], the mercury and cadmium elements have been used in combination with pnicogen in order to obtain new semiconducting compounds with unique physical properties and abundant structural features. And a new quaternary cadmium and mercury pnictidehalide semiconductor ($Hg_2Cd_2As_2Br$)Br, which consists of a 3-D cationic host network with the channels being occupied by discrete Br anions, has been obtained [1e].

In the present work, as a view to preparation of new host–guest compounds based on the second type of the topology, we selected cadmium atom as coordination center for the tetrahedral guests and the halogen atoms from Cl to I. However, we succeeded only in synthesizing a new quaternary phase, $(Hg_2As)_2(CdI_4)$ (**1**). Herein, we report the synthesis, crystal and electronic band structures, and optical properties of the new supramolecular complex.

2. Experimental and computational procedures

2.1. Synthesis and analyses

Single Crystals of **1** were initially prepared by the solid-state reaction of a mixture of HgI_2 (1 mmol, 455 mg), Cd (0.5 mmol, 56 mg), CdI_2 (0.5 mmol, 183 mg), and As (0.5 mmol, 37 mg) at 320 °C. The starting materials were ground into fine powders in an agate mortar and pressed into a pellet, followed by being loaded into a Pyrex tube, evacuated to 1×10^{-4} Torr, and flame-sealed. The tube was placed into a computer-controlled furnace, heated from the room temperature to 200 °C at a rate of 50 °C/h, kept at 200 °C for 4 h. The tube was then heated to 320 °C at 20 °C/h, kept at 320 °C for 120 h, and then slowly cooled down to 100 °C at a rate of 2 °C/h, it was finally cooled down to the room temperature over 4 h. A crop of black crystals of **1** that is stable in air was obtained. Semiquantitative microscope element analysis on several single crystals of **1** was performed on a field-emission scanning electron microscope (FESEM, JSM6700F) equipped with an energy dispersive X-ray spectroscope (EDS, Oxford INCA), which confirmed the presence of Hg, Cd, As and I in the approximate molar ratio 3.9:1.0:2.0:3.9. No other elements were detected. The exact composition was established from the X-ray structure determination. After structural analysis, a black crystalline sample of **1** was then obtained quantitatively by the reaction of a mixture of Hg_2I_2/Cd/As in a molar ratio of 2/1/2 at 320 °C for 120 h. The purity of the black crystalline sample was confirmed by XRD powder diffraction study.

2.2. X-ray single crystal structure determination

A black single crystal of **1** was mounted on a glass fiber for the X-ray diffraction analysis. Data was collected on a Rigaku Mercury CCD diffractometer equipped with a graphite-monochromated Mo$K\alpha$ radiation ($\lambda = 0.71073$ Å) at 293 K. The intensity data were collected with an ω scan technique and corrected for *LP* factors as well as for absorption by the multiscan method [7]. The structure was solved by direct methods and refined on F^2 with full-matrix least-squares techniques using Siemens SHELXTL version 5 package of crystallographic software [8]. The final refinements included anisotropic displacement parameters for all atoms and a secondary extinction correction. The crystallographic data of **1** is listed in Table 1. The atomic coordinates and thermal parameters are listed in Table 2. Selected bond lengths and bond angels are given in Table 3.

2.3. Physical measurements

The powder XRD pattern was collected with a Rigaku DMAX2500 diffractometer at 40 kV and 100 mA for Cu$K\alpha$ ($\lambda = 1.5406$ Å) with a scan speed of 5°/min at room temperature. The simulated pattern was produced using the Mercury program and single-crystal reflection data. Fig. S1 gives the powder XRD pattern of **1,** which corresponds well with the simulated one, conforming the high purity of the prepared sample. Thermogravimetric analysis (TGA) and differential scanning calorimetry were performed on a Netzsch Sta449C thermoanalyzer under a N_2 atmosphere in the range of 30–750 °C at a heating rate of 10 °C/min. Fig. S2 shows that no weight changes in **1** until 180 °C.

The UV–vis spectrum of **1** was recorded at the room temperature on a computer-controlled PE Lambda 35

Table 1
Crystal data and structure refinement parameters for **1**

Formula	$[Hg_2As]_2(CdI_4)$
Formula weight ($g\,mol^{-1}$)	1572.20
Crystal size (mm^3)	$0.10 \times 0.10 \times 0.10$
T (K)	293(2)
λ (Mo$K\alpha$, Å)	0.71073
Crystal system	Monoclinic
Space group	$P2_1$
a (Å)	7.945(4)
b (Å)	12.934(6)
c (Å)	8.094(4)
β (°)	116.898(1)
V ($Å^3$)	741.7(6)
Z	2
D_{calcd} ($g\,cm^{-3}$)	7.040
μ (mm^{-1})	55.371
$F(000)$	1292
θ range (°)	3.15–25.03
Limiting indices	$-8 \leqslant h \leqslant 9$; $-15 \leqslant k \leqslant 13$; $-9 \leqslant l \leqslant 8$
Reflections collected	4881
Independent reflections	2488 ($R_{int} = 0.0389$)
R^a	0.0356
$R_w{}^b$	0.0742
GOF on F^2	1.000
$\Delta\rho_{max}$ and $\Delta\rho_{min}$ ($e\,Å^{-3}$)	2.305 and −1.503

[a] $R = \sum||F_o|-|F_c||/\sum|F_o|$.
[b] $R_w = \{\sum[w(F_o^2-F_c^2)^2]/\sum[w(F_o^2)^2]\}^{1/2}$.

Table 2
Atomic coordinates and equivalent isotropic displacement parameters for **1**

Atom	*x*	*y*	*z*	U_{eq}[a]
Hg(1)	0.6725(2)	0.20971(7)	1.3314(1)	0.0336(3)
Hg(2)	0.5275(2)	0.48065(8)	1.4498(2)	0.0402(3)
Hg(3)	0.5120(2)	0.44385(8)	0.94637(1)	0.0390(3)
Hg(4)	1.0266(2)	0.45169(9)	1.4321(2)	0.0402(3)
I(1)	0.2885(2)	0.1896(1)	0.9005(2)	0.0349(4)
I(2)	−0.3281(3)	0.2556(1)	0.7437(2)	0.0388(5)
I(3)	0.1321(3)	0.1908(1)	1.3754(2)	0.0370(4)
I(4)	−0.1085(3)	−0.0445(1)	0.9487(3)	0.0439(5)
Cd(1)	0.0025(2)	0.1660(1)	1.0006(2)	0.0206(4)
As(1)	0.6892(4)	0.3986(2)	1.2817(3)	0.0232(6)
As(2)	0.6503(4)	0.0193(2)	1.3710(3)	0.0230(6)

[a] U_{eq} is defined as one third of the trace of the orthogonalized U_{ij} tensor.

Table 3
Selected bond distances (Å) and bond angles (°) for **1**[a]

Hg(1)–As(2)	2.500(3)	Hg(4)–As(1)	2.487(3)
Hg(1)–As(1)	2.489(3)	Hg(4)–As(2)#3	2.489(3)
Hg(2)–As(1)	2.491(3)	I(1)–Cd(1)	2.753(3)
Hg(2)–As(2)#1	2.491(3)	I(2)–Cd(1)	2.761(2)
Hg(3)–As(2)#2	2.493(3)	I(3)–Cd(1)	2.745(3)
Hg(3)–As(1)	2.497(3)	I(4)–Cd(1)	2.834(3)
As(2)–Hg(1)–As(1)	178.29(9)	Hg(4)–As(1)–Hg(2)	108.8(1)
As(1)–Hg(2)–As(2)#1	166.36(9)	Hg(1)–As(1)–Hg(2)	104.6(1)
As(2)#2–Hg(3)–As(1)	170.46(9)	Hg(4)–As(1)–Hg(3)	114.8(1)
As(1)–Hg(4)–As(2)#3	168.98(10)	Hg(1)–As(1)–Hg(3)	111.1(1)
I(3)–Cd(1)–I(1)	111.44(8)	Hg(2)–As(1)–Hg(3)	108.5(1)
I(3)–Cd(1)–I(2)	122.45(8)	Hg(1)–As(2)–Hg(3)#5	106.68(9)
I(1)–Cd(1)–I(2)	111.26(9)	Hg(4)#4–As(2)–Hg(3)#5	115.2(1)
I(3)–Cd(1)–I(4)	102.23(7)	Hg(1)–As(2)–Hg(2)#6	111.3(1)
I(1)–Cd(1)–I(4)	107.81(8)	Hg(4)#4–As(2)–Hg(2)#6	104.4(1)
I(2)–Cd(1)–I(4)	99.49(8)	Hg(3)#5–As(2)–Hg(2)#6	110.9(1)
Hg(4)–As(1)–Hg(1) × 2	108.4(1)		

[a] Symmetry transformations used to generate equivalent atoms: #1—$x+1, y+1/2, -z+3$; #2—$x+1, y+1/2, -z+2$; #3—$x+2, y+1/2, -z+3$; #4—$x+2, y-1/2, -z+3$; #5—$x+1, y-1/2, -z+2$; #6—$x+1, y-1/2, -z+3$.

UV–vis spectrometer equipped with an integrating sphere in the wavelength range 200–1100 nm. A $BaSO_4$ plate was used as a reference, on which the finely ground powder of the sample was coated. The absorption spectrum was calculated from reflection spectrum by the Kubelka-Munk function [9]: $\alpha/S = (1-R)^2/2R$, where α is the absorption coefficient, S is the scattering coefficient that is practically wavelength independent when the particle size is larger than 5 μm, and R is the reflectance. The energy gap was determined as the intersection point between the energy axis at the absorption offset and the line extrapolated from the linear portion of the absorption edge in the α/S versus E (eV) plot. The IR spectrum was recorded by using a Nicolet Magana 750 FT-IR spectrophotometer in the range of 4000–400 cm^{-1}. A powdery sample was pressed into pellets with KBr. The IR spectrum is given in Fig. S3.

2.4. Computational procedures

The crystallographic data of the present compound determined by X-ray was used to calculate its electronic band structure. The calculation of electronic band structure along with the density of states (DOS) was performed with the CASTEP code [10] based on the density functional theory (DFT) using a plane-wave expansion of the wave functions and norm-conserving pseudopotential [11], in which the orbital electrons of I-$5s^25p^5$, As-$4s^24p^3$, Cd-$4d^{10}5s^2$, and Hg-$5d^{10}6s^2$ were treated as valence electrons. We used the generalized gradient approximation (GGA) in the scheme of Perdew–Burke–Eruzerhof (PBE) to describe the exchange and correlation potential, since the GGA was more widely used to calculate and analyze band structures of the inorganic compounds than the local-density approximation (LDA) [12]. To confirm the convergence of our calculations, we carefully investigated the

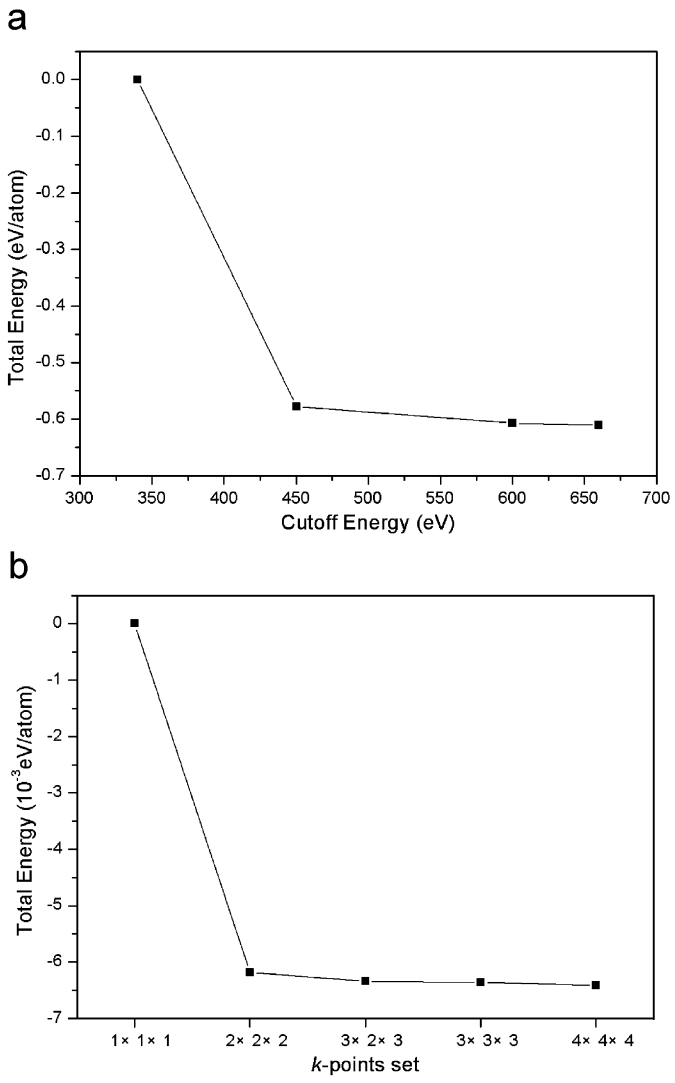

Fig. 1. Convergence of the total energy of **1** at different computational parameters. (a) Total energy versus the cutoff energy for the *k*-point mesh of 3 × 2 × 3. (b) Total energy versus the *k*-point mesh for the cutoff energy of 450 eV.

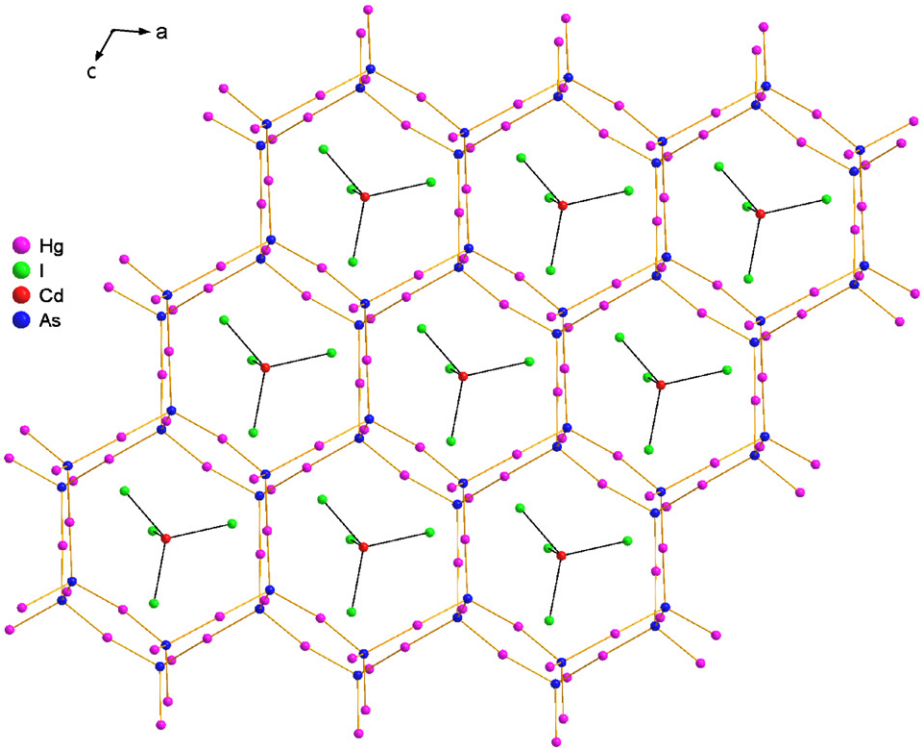

Fig. 2. Projection of the crystal structure of **1** along the *b*-axis.

dependences of the total energy on the cutoff energy and the *k*-point set mesh according to the Monkhorst-Pack grid. As shown in Fig. 1, when the *k*-point set mesh is fixed in $3 \times 2 \times 3$, the change in total energy is less than 0.05 eV when the cutoff energy is higher than 450 eV; on the other hand, when the cutoff energy is fixed in 450 eV, the convergence in total energy is very well when the *k*-point set mesh is beyond $3 \times 2 \times 3$. In consideration of computational cost, we choose the cutoff energy to be in 450 eV, and the Brillouin-zone sampling mesh parameters for the *k*-point set are $3 \times 2 \times 3$.

3. Results and discussion

The crystal structure of **1** is characterized by a tridymite-like three-dimensional cationic framework composed of mercury and arsenic atoms. Among the framework, the mercury atoms have nearly linear coordination with a mean As–Hg–As bond angle of 171.1°, while the arsenic atoms possess an almost regular tetrahedral coordination by four mercury atoms, and these tetrahedra share corners each other through mercury atoms to form the cationic network with channels along the *b* direction (Fig. 2). As for the guest anions, each the cadmium atoms is coordinated by four iodide atoms to form a nearly regular tetrahedron, which are embedded in the channels with the shortest Hg–I bond distance being 3.391(2) Å.

There are four crystallographic independent mercury atoms in the structure of **1**. Analogues to the compound $(Hg_2As)_2(ZnI_4)$ [5b], the mercury atoms are all almost

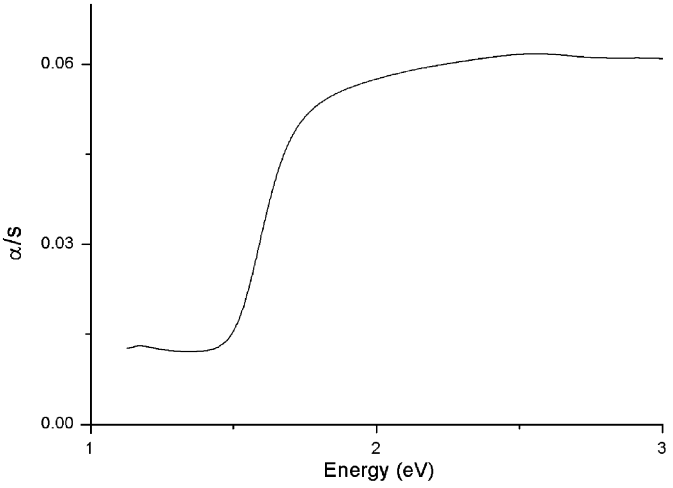

Fig. 3. Diffuse reflectance spectrum of **1**.

linearly coordinated by two arsenic atoms in the present compound. The Hg–As bond distances range from 2.487(3) to 2.500(3) Å, which lie in the normal range of the Hg–As separations in mercury arsenidehalides [13]. The Cd–I bond distances range from 2.753(3) to 2.834(3) Å, which are shorter than those found in cadmium iodides [14] and cadmium pnictidehalides [15].

The host–guest distances in **1** are significantly longer than expected for covalent bonding, which is the feature of supramolecular ensembles. The separations between the iodine atoms of the guest anions and the mercury atoms in

the host framework range from 3.39 to 3.68 Å, which are much longer than the normal Hg–I covalent bond distance (2.83 Å) and shorter than the sum of van de Waals radii of Hg and I atoms. Thus, the host–guest supramolecular interactions fix the tetrahedral anions to their specific position so that no position or rotational disorder is observed for them, which is also found in the literatures [1a,b,2b,c].

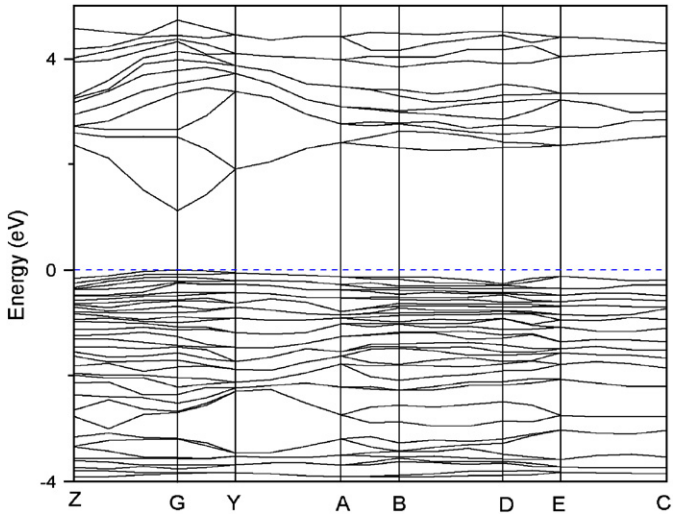

Fig. 4. The band structure of **1** (the bands is shown only between −4 and 5 eV for clarity, and the dashed line indicates the position of the Fermi level).

The diffuse reflectance spectrum of **1** reveals the presence of an optical gap of 1.45 eV (Fig. 3), which suggests that the present compound is semiconductor and consistent with its color. The energy gap of **1** is approximate to those of CdTe (1.44 eV), GaAs (1.43 eV), and $CuInS_2$ (1.55 eV), all of which are highly efficient photovoltaic materials [16]. Thus we can suppose that the present compound may become potential material for the efficient absorption of solar radiation in solar cell applications. The IR spectrum of **1** shows no obvious absorption in the range of 4000–400 cm^{-1}, which supports the idea that the compound may be potentially used as window materials for laser delivery media and infrared transmitting for optical fiber applications in telecommunication [17].

The calculated band structure of **1** along high symmetry points of the first Brillouin zone is plotted in Fig. 4, where the labeled *k*-points are present as *Z* (0.0, 0.0, 0.5), *G* (0.0, 0.0, 0.0), *Y* (0.0, 0.5, 0.0), *A* (−0.5, 0.5, 0.0), *B* (−0.5, 0.0, 0.0), *D* (−0.5, 0.0, 0.5), *E* (−0.5, 0.5, 0.5), and *C* (0.0, 0.5, 0.5). It is found that the top of valence bands (VBs) has small dispersion, whereas the bottom of conduction bands

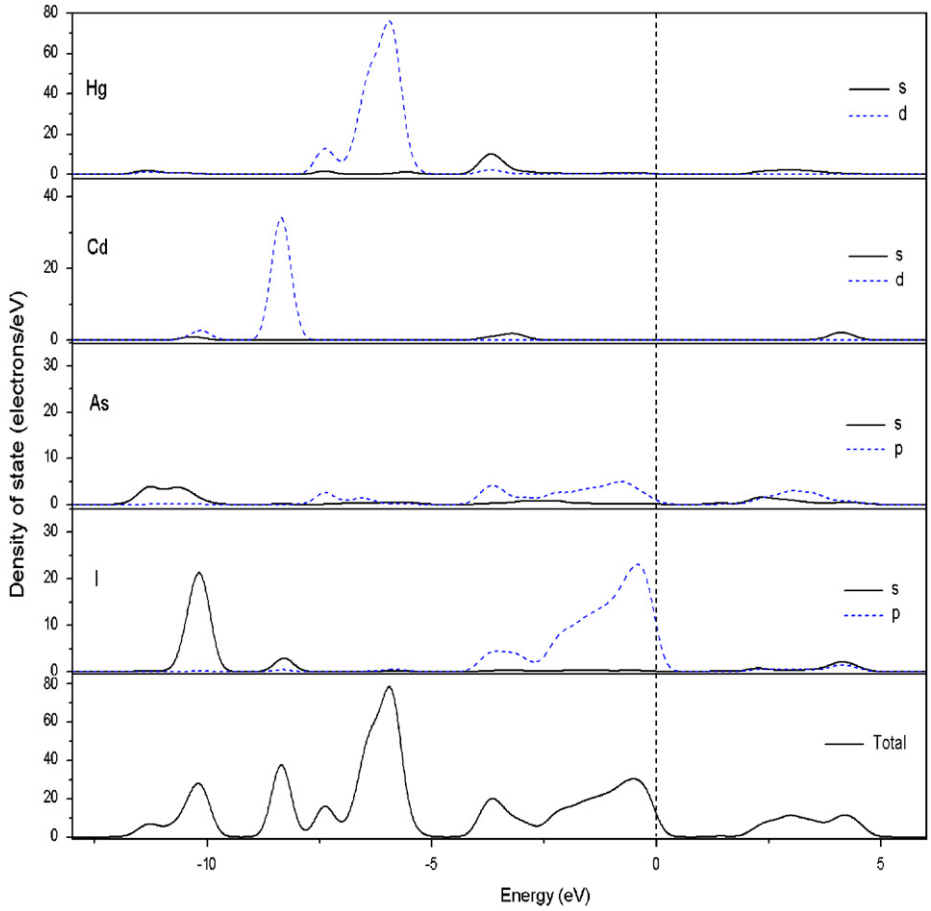

Fig. 5. The total and partial DOS of **1**. The position of the Fermi level is set at 0 eV.

(CBs) has big dispersion. The lowest energy (1.11 eV) of CBs and the highest energy (0.00 eV) of VBs are both localized at *G* point. According to our calculations, the solid-state compound **1** thus shows a semiconducting character with a direct band gap of 1.11 eV, which is comparable with the experimental value (1.45 eV). The bands can be assigned according to total and partial densities of states (DOS), as plotted in Fig. 5. The Hg-5*d*, Cd-4*d* and I-5*s* states, mixing with small As-4*s* and As-4*p* states, create the VBs localized between −12.5 and −5.0 eV. The VBs between −5.0 eV and the Fermi level (0.0 eV) are mostly formed by I-5*p* and As-4*p* states mixing with a small amount of the Cd-5*s* and Hg-6*s* states, while the CBs between 1.1 and 5.0 eV are almost contribution from Cd-5*s*, Hg-6*s*, As-4*p*, and I-5*s* states hybridized with a small amount of As-4*s* and I-5*p* states. Accordingly, it can be considered that the optical absorption of **1** is mainly ascribed to the charge transitions from I-5*p* and As-4*p* to Cd-5*s* and Hg-6*s* states.

Furthermore, we calculated the atomic site and angular momentum projected DOS of **1** to elucidate the nature of the electronic band structure and chemical bonds. As shown in Fig. 5, it can be observed that the density and shape of As-4*p* state is similar to that of Hg-6*s* state between −5.0 and −2.5 eV, while the DOS of I-5*p* is higher than that of Cd-5*s* state, which indicates that there are covalent interactions in the bond of Hg–As and weak covalent interactions in the Cd–I bond.

Semiempirical population analysis allows for a more quantitative bond analysis. The calculated bond orders of the Cd–I, Hg–As and Hg–I are from −0.01 to 0.36, 0.51 to 0.71, and −0.29 to −0.01 e in a unit cell of **1** (pure covalent single bond order is generally 1.0 e), respectively. Accordingly, it indicates that the Hg–As bond is mainly covalent character, whereas the Cd–I bond is mainly ionic character. And there are only weak interactions between Hg and I, which are in good agreement with the crystal structure of **1**.

4. Conclusion

In the present work, a new quaternary supramolecular complex $(Hg_2As)_2(CdI_4)$ has been synthesized and characterized. The diffuse reflectance spectrum of **1** reveals the presence of an optical gap of 1.45 eV, and the IR spectrum of **1** shows no obvious absorption in the range of 4000–400 cm^{-1}. The calculations of the electronic band structure along with DOS indicate that the present compound is a semiconductor with a direct band gap, and that the optical absorption is mainly originated from the charge transitions from I-5*p* and As-4*p* to Cd-5*s* and Hg-6*s* states. The DOS and semiempirical population analysis indicate that the Hg–As and Cd–I bonds are mainly covalent character and ionic character, respectively, while there are only weak interactions between Hg and I, which are in good agreement with the crystal structure of **1**.

5. Supporting information available

Experimental and simulated powder X-ray diffraction pattern, TG and DSC curve, IR spectrum, and molecular structure figures of **1** are available. Further details of the crystal structure investigation(s) can be obtained from the Fachinformationszentrum Karlsruhe, 76344 Eggenstein-Leopoldshafen, Germany, (fax: (49) 7247 808 666; e-mail: crysdata@fiz-karlsruhe.de) on quoting the depository number CSD-416973.

Acknowledgment

We gratefully acknowledge the financial support of the NSF of China (20571075, 20521101), the NSF for Distinguished Young Scientist of China (20425104), and the NSF of CAS (KJCX2-SW-h05).

References

[1] O.S. Oleneva, A.V. Olenev, E.V. Dikarev, A.V. Shevelkov, Eur. J. Inorg. Chem (2004) 4006–4010;
A.V. Olenev, O.S. Oleneva, M. Lindsjö, L.A. Kloo, A.V. Shevelkov, Chem. Eur. J. (2003) 3201–3208;
O.S. Oleneva, A.V. Olenev, T.A. Shestimerova, A.I. Baranov, E.V. Dikarev, A.V. Shevelkov, Inorg. Chem. 44 (2005) 9622–9624;
A.V. Olenev, A.V. Shevelkov, Angew. Chem. Int. Ed. 40 (2001) 2353–2354;
J.-P. Zou, G.-C. Guo, W.-T. Chen, X. Liu, M.-L. Fu, Z.-J. Zhang, J.-S. Huang, Inorg. Chem. 45 (2006) 6365–6369;
J. Beck, S. Hedderich, K. Köllisch, Inorg. Chem. 154 (2000) 5847–5850;
A.V. Olenev, A.I. Baranov, A.V. Shevelkov, B.A. Popovkin, Eur. J. Inorg. Chem. 1 (2000) 265–270.

[2] H. Puff, M. Grönke, B. Kilger, P. Möltgen, Z. Anorg, Allg. Chem. 518 (1984) 120–124;
J. Beck, S. Hedderich, U. Neisel, J. Solid State Chem. 154 (2000) 350–355;
A.V. Shevelkov, M.M. Shatruk, Russ. Chem. Bull. Int. Ed. 50 (2001) 337–362.

[3] H. Puff, M. Grönke, B. Kilger, P. Möltgen, Z. Anorg, Allg. Chem. 518 (1984) 120–124;
J. Beck, S. Hedderich, U. Neisel, J. Solid State Chem. 154 (2000) 350–355;
A.V. Shevelkov, M.M. Shatruk, Russ. Chem. Bull. Int. Ed. 50 (2001) 337–362.

[4] A.V. Shevelkov, M.Y. Mustyakimov, E.V. Dikarev, B.A. Popvkin, J. Chem. Soc., Dalton Trans. 1 (1996) 147–149.

[5] A.V. Olenev, A.V. Shevelkov, B.A. Popovkin, Zh. Neorgan. Khim. 44 (1999) 1853–1856;
A.V. Olenev, A.V. Shevelkov, B.A. Popovkin, Zh. Neorgan. Khim. 44 (1999) 1814–1816.

[6] R. Laiho, A.V. Lashkul, K.G. Lisunov, E. Lähderanta, M.O. Safonchik, M.A. Shakhov, J. Phys.: Condens. Matter 16 (2004) 333–342;
R. Laiho, A.V. Lashkul, K.G. Lisunov, E. Lähderanta, M.O. Safonchik, M.A. Shakhov, Semicond. Sci. Technol. 19 (2004) 602–609.

[7] R. Laiho, A.V. Lashkul, K.G. Lisunov, E. Lähderanta, M.O. Safonchik, M.A. Shakhov, J. Phys.: Condens. Matter 16 (2004) 333–342;
R. Laiho, A.V. Lashkul, K.G. Lisunov, E. Lähderanta, M.O. Safonchik, M.A. Shakhov, Semicond. Sci. Technol. 19 (2004) 602–609.

[8] Siemens SHELXTL^{TM} Version 5 Reference Manual, Siemens Energy & Automation Inc., Madison, Wisconsin, 1994.
[9] W.W. Wendlandt, H.G. Hecht, Reflectance Spectroscopy, Interscience Publishers, New York, 1966;
G. Kortüm, Reflectance Spectroscopy, Springer, New York, 1969.
[10] W.W. Wendlandt, H.G. Hecht, Reflectance Spectroscopy, Interscience Publishers, New York, 1966;
G. Kortüm, Reflectance Spectroscopy, Springer, New York, 1969.
[11] D.R. Hamann, M. Schluter, C. Chiang, Phys. Rev. Lett. 43 (1979) 1494–1497.
[12] M. Segall, P. Linda, M. Probert, C. Pickard, P. Hasnip, S. Clark, M. Payne, J. Phys.: Condens. Matter 14 (2002) 2717–2744;
J.P. Perdew, K. Burke, M. Ernzerhof, Phys. Rev. Lett. 77 (1996) 3865–3867;
S.-P. Huang, W.-D. Cheng, D.-S. Wu, X.-D. Li, Y.-Z. Lan, F.-F. Li, J. Shen, H. Zhang, Y.-J. Gong, J. Appl. Phys. 99 (2006) 0135161–0135164;
Y.-C. Zhang, W.-D. Cheng, D.-S. Wu, H. Zhang, D.-G. Chen, Y.-J. Gong, Z.-G. Kan, Chem. Mater. 16 (2004) 4150–4159;
S.-P. Huang, D.-S. Wu, J. Shen, W.-D. Cheng, Y.-Z. Lan, F.-F. Li, H. Zhang, Y.-J. Gong, J. Phys.: Condens. Matter 18 (2006) 5535–5544;
J. Zhu, W.-D. Cheng, D.-S. Wu, H. Zhang, Y.-J. Gong, H.-N. Tong, J. Solid State Chem. 179 (2006) 597–604.
[13] A.V. Shevelkov, E.V. Dikarev, B.A. Popvkin, J. Solid State Chem. 126 (1996) 324–327;
A.V. Shevelkov, E.V. Dikarev, B.A. Popvkin, Zh. Neorgan. Khim. 40 (1995) 1496–1501.
[14] R.M. Bozorth, J. Am. Chem. Soc. 44 (1922) 2232–2236;
P.C. Jain, M.A. Wahab, G.C. Trigunayat, Acta Crystallogr. B 34 (1978) 2685–2689;
B. Palosz, Acta Crystallogr. C 39 (1983) 521–528.
[15] J. Gallay, G. Allais, A. Deschanvres, Acta Crystallogr. B 31 (1975) 2274–2276;
R.E. Marsh, F.H. Herbstein, Acta Crystallogr. B 44 (1988) 77–88;
A. Rebbah, J. Yazbeck, R. Lande, A. Deschanvres, Mater. Res. Bull. 16 (1981) 525–533.
[16] C.H. Champness, Phosphorous Sulfur Relat. Elem. 38 (1988) 385–397;
R.H. Dube, PhotoVoltaic Materials, Imperial College Press, 1998, p. 135;
P. Dürichen, W. Bensch, Eur. J. Solid State Inorg. Chem. 34 (1997) 1187–1190.
[17] J.A. Harrington, Infrared Fibers and Their Applications, SPIE Press, Bellingham, WA, 2004;
D. Marchese, M. De Sario, A. Jha, A.K. Kar, E.C. Smith, J. Opt. Soc. Am. B 15 (1998) 2361–2370.